



## Drought decreases streamflow response to precipitation especially in arid regions

3

Alessia Matanó<sup>1</sup>, Raed Hamed<sup>1</sup>, Manuela I. Brunner<sup>2,3,4</sup>, Marlies H. Barendrecht<sup>5</sup>, Anne F. Van Loon<sup>1</sup>

6 <sup>1</sup> Institute for Environmental Studies, Vrije Universiteit Amsterdam, Amsterdam, The Netherlands

<sup>2</sup> Institute for Atmospheric and Climate Science, ETH Zurich, Zurich, Switzerland

9 <sup>3</sup> WSL Institute for Snow and Avalanche Research SLF, Swiss Federal Institute for Forest, Snow and  
Landscape Research WSL, Davos Dorf, Switzerland

<sup>4</sup> Climate Change, Extremes and Natural Hazards in Alpine Regions Research Center CERC, Davos  
Dorf, Switzerland

12 <sup>5</sup> Department of Geography, King's College London, London, United Kingdom

Corresponding author: Alessia Matanó ([alessia.matano@vu.nl](mailto:alessia.matano@vu.nl))

15

### Abstract

18 Persistent drought conditions may alter catchment response to precipitation, both during and after the  
drought period, hindering accurate streamflow forecasting of high flows and floods. Yet, the influence  
of drought characteristics on the catchment response to precipitation remains unclear. In this study, we  
use a comprehensive dataset of global observations of streamflow and remotely sensed precipitation,  
21 soil moisture, total water storage and normalized difference vegetation index (NDVI). Using  
multivariate statistics on 4487 catchments with a stationary streamflow-to-precipitation ratio, we  
investigate the influence of drought on fluctuations of streamflow sensitivity to precipitation. Our  
24 analysis shows that generally droughts with streamflow or soil moisture anomalies below the 15th  
percentile lead to around 20% decrease in streamflow sensitivity to precipitation during drought  
compared to the historical norm, with up to a 2% decrease one year after the drought. Negative NDVI  
27 anomalies are the only exception, resulting in a 3% increase in sensitivity. These effects are more  
pronounced when droughts are longer and more severe. Most changes were found in arid and warm-  
temperate regions, whereas snow-influenced regions exhibit less sensitivity changes due to drought. In  
30 addition, we used step-change analyses on 1107 catchments with non-stationary streamflow-to-  
precipitation ratio to identify significant abrupt shifts on the timeseries, examining the role of drought  
in driving these shifts. This analysis revealed both positive and negative shifts in streamflow sensitivity  
33 after severe and persistent drought conditions regardless of climate and catchment characteristics.  
Positive shifts occur only when the drought propagated through the hydrological system after extended



dry periods, while negative shifts are usually linked to shorter, intense dry periods. This study sheds  
36 light on the importance of considering climate characteristics in predicting dynamic catchment response  
to precipitation during and after persistent drought conditions.

39

### 1. Introduction

Drought is known to exert significant influence on catchment hydrological behaviour. Events such as  
42 the mega drought in Chile (Alvarez-Garreton et al. 2021; Garreaud et al. 2017), the millennium drought  
in Australia (Saft, Peel, Western, and Zhang 2016) and the 2011 Texas drought (Klockow et al. 2018)  
have resulted in substantial changes in vegetation productivity and type, soil hydraulic properties,  
45 surface water-groundwater interactions and water storage. Yet, understanding the extent of drought  
influence on catchment hydrologic response remains a crucial question with significant implications for  
enhancing hydrological prediction under future conditions.

48 Researchers have studied the impact of persistent drought conditions on catchment response using  
linear-regression approaches (Avanzi et al. 2020; Liu et al. 2022; Massari et al. 2022; Peterson et al.  
2021; Saft et al. 2015; Saft, Peel, Western, and Zhang 2016; Wu et al. 2021) and water balance models  
51 (Liu et al. 2023; Maurer et al. 2022; Pan et al. 2020), registering a shift in rainfall-runoff relationships  
during long drought periods. According to Saft et al. (2015, 2016), persistent drought conditions in  
Australia's multi-year drought resulted in significantly less than expected runoff for some of the basins  
54 studied. This has been mainly attributed to reduced groundwater levels and hence, initial precipitation  
is used for replenishing water storage before runoff can occur. This process is prevalent in arid regions  
with high surface water-groundwater connection and large soil thickness, highlighting the linkage  
57 between changes in rainfall-runoff and catchment characteristics during persistent drought conditions.  
Peterson et al. (2021) have shown that rainfall-runoff shifts can persist after drought, in this case due to  
an increase in the fraction of precipitation going to evapotranspiration. Similarly to the Australian study,  
60 Avanzi et al. (2020) and Maurer et al. (2022) have identified less runoff during droughts in California  
than expected, attributing this to nonlinear feedback mechanisms between evapotranspiration and  
storage. Only a few catchments showed runoff increases mainly explained by catchment buffer  
63 capacities such as soil storage and snow-to-rain transitions.

Despite these findings, uncertainties remain on the specific catchment characteristics that contribute to  
vulnerability to drought-induced changes in the Q-P relationship, as well as the drought conditions that  
66 lead to these changes and the direction of the change (e.g., increase or decrease). Previous studies relied  
on samples with limited variability in catchment characteristics, with a large focus on natural catchments  
in Australia (Liu et al. 2021; Pan et al. 2020; Peterson et al. 2021; Saft et al. 2015; Saft, Peel, Western,  
69 and Zhang 2016) and California (Avanzi et al. 2020; Bales et al. 2018; Maurer et al. 2022). Furthermore,



analyses of changes in rainfall-runoff relationships have primarily focused on the effects of meteorological droughts (Liu et al. 2021; Massari et al. 2022; Pan et al. 2020; Peterson et al. 2021; Saft et al. 2015; Saft, Peel, Western, and Zhang 2016), neglecting other drought types and failing to assess the effect of drought severity and duration on changes in the rainfall-runoff relationship.

Here, we analysed the temporal dynamics of the streamflow sensitivity to precipitation (computed as the ratio between annual streamflow and precipitation) in approximately 5000 catchments across the world. Specifically, we addressed the following questions: (1) how do drought characteristics (types, duration and severity) influence streamflow sensitivity to precipitation in general and in different hydro-climatic regions across the globe? and (2) when and where do abrupt changes in streamflow sensitivity to precipitation occur and how do those changes align with drought periods? To address these research questions, we first divided the catchments according to stationary and non-stationary streamflow-precipitation ratio timeseries. Then, we employed mixed effects panel data models on stationary streamflow-precipitation timeseries to answer RQ1 and step-change analysis by using threshold regression models on non-stationary streamflow-precipitation timeseries to answer RQ2.

84

## 2. Methodology

### 2.1 Data preparation and drought detection

87 We identified a large sample of 5590 catchments, whose hydrometeorological timeseries span 25 to 34 years from 1980 to 2016. We compiled observed streamflow data from the Global Streamflow Indices and Metadata Archive (GSIM) database (Do et al. 2018; Gudmundsson et al. 2018). Using the catchment delineations in the GSIM dataset, we derived a set of hydro-climatic time series using Multi-Source Weighted-Ensemble Precipitation (MSWEP; Beck et al. 2019) for the precipitation sum over the catchment, the Global Land Evaporation Amsterdam Model (GLEAM; Martens et al. 2017) for surface (0 – 5 cm depth) and root zone (0 – 250 cm depth) soil moisture, the Gravity Recovery And Climate Experiment (GRACE; Boergens, Doblslaw, and Dill 2019) for total water storage, Landsat for surface water extent (Donchyts et al. 2016; Earth Resources Observation and Science (EROS) Center 2022), and STAR - Global Vegetation Health Products for the normalized difference vegetation index (NDVI; NOAA 2022). These datasets and their post-processing are explained in more detail in Table S1 of the Supplementary Information and in Matanó et al. (2024).

99 From average daily streamflow and total precipitation per month, we derived annual average daily streamflow (mm/day) and annual average daily precipitation (mm/day) for each catchment. As such, we assume that the storage change is negligible over an annual time scale. Data aggregation to a yearly scale was based on water years, defined for each catchment as the 12-month period beginning in the month of the lowest average monthly streamflow (Wasko, Nathan, and Peel 2020). We then applied a Box-Cox transformation (Sakia 1992) to normalize the skewed yearly streamflow distribution (Saft et

102



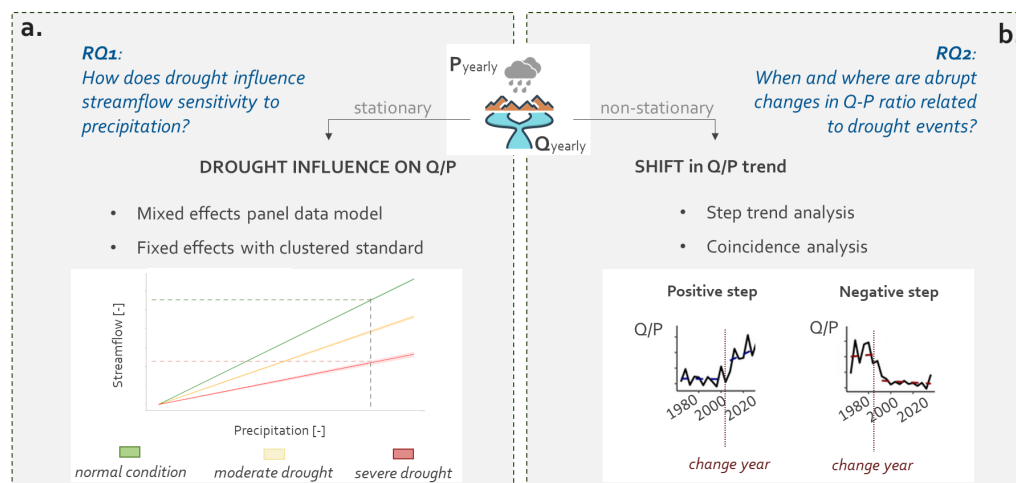
105 al. 2015; Saft, Peel, Western, and Zhang 2016). This allowed us to obtain an approximately linear  
rainfall-runoff relationship, thereby facilitating the application of various statistical methods. Further,  
the Box–Cox transformation allowed us to overcome the issue of applying a log-transformation to  
108 streamflow timeseries with zero flow (e.g., ephemeral or intermittent rivers; Santos, Thirel, and Perrin  
2018). We then computed yearly streamflow-to-precipitation (Q-P) ratio timeseries for each catchment.

Drought events were detected using a variable threshold-level approach for perennial rivers (Van Loon  
111 2015) and, a combined threshold-level and consecutive dry period method for ephemeral rivers (Van  
Huijgevoort et al. 2012; we refer to Matanó et al. 2024, for details on the method used for drought  
detection). We employed monthly-varying exceedance probabilities of the 15th, 10th, 5th, and 1<sup>st</sup>  
114 percentiles on precipitation, soil moisture, streamflow, total water storage, and surface water extent  
monthly timeseries. Additionally, NDVI anomalies per catchment were analysed to understand  
vegetation health and water flux dynamics. Drought characteristics were summarized at a yearly scale,  
117 by calculating maximum severity (defined as the difference between observed values and a predefined  
threshold), maximum cumulative severity (sum of consecutive severity across years), sum of severity,  
maximum cumulative duration (defined as the number of consecutive months in which observations are  
120 under a certain threshold), and sum of months under drought for each water year. These metrics were  
computed for each variable and were also aggregated for three types of drought: meteorological drought  
(based solely on precipitation data), soil moisture drought (incorporating surface and root zone soil  
123 moisture), and hydrological drought (taking into account streamflow, surface water extent, and total  
water storage).

## 126 **2.2 Stationarity test and research framework**

We tested the stationarity over time of yearly streamflow-to-precipitation ratios (Q-P) using the  
Augmented Dickey-Fuller (ADF) test (Paparoditis and Politis 2018), with a significance level set at  
129 0.05. This test primarily assesses whether the mean of the streamflow-precipitation relationship  
remained consistent over time, regardless of fluctuations around it.

We then divided our catchments in two groups: catchments with stationary Q-P timeseries and those  
132 with non-stationary Q-P time series. For stationary Q-P timeseries (ADF test  $p\_value < 0.05$ ), we  
evaluated the influence of drought on streamflow sensitivity to precipitation by employing a mixed-  
effects panel data model (Gelman and Hill 2007; Figure 1a). For Q-P timeseries displaying non-  
135 stationary behaviour (ADF test  $p\_value > 0.05$ ), we identified potential step-changes in the streamflow-  
to-precipitation ratio and their coincidence with drought conditions (Figure 1b). With the use of these  
two different approaches, we analysed both the dynamic influence of drought on stationary Q-P time  
138 series (RQ1) and the more structural changes during drought in non-stationary series (RQ2).



141 **Figure 1.** Research framework. (a) Methodology applied to investigate the influence of drought on streamflow  
142 sensitivity to precipitation. (b) Methodology applied to identify step changes in the Q-P ratio trend and system  
143 state conditions (e.g., anomaly presence) during the change year.

### 144 2.3 Panel data models for stationary Q-P timeseries

145 We used a mixed-effects panel data model (Gelman and Hill 2007) on 4487 catchments with a stationary  
146 streamflow-to-precipitation ratio to explore the influence of drought conditions on the variability of  
147 streamflow sensitivity to precipitation over time. The mixed-effects model offers several advantages.  
148 First, it estimates both the general effect of drought characteristics on streamflow sensitivity to  
149 precipitation across all catchments (fixed effect) and the variation of this effect between catchments  
150 (random effect). Second, this model is ideal for analysing hydrological units, as it can account for  
151 potential correlations between "nested" basins (Levy et al. 2018).

152 We ran two mixed-effects panel data models whose formulation is presented in Equations 1 and 4, to  
153 assess the impact of various drought types on the streamflow-to-precipitation ratio, accounting for  
154 different data availability. Before employing these formulations, we tested several drought metrics such  
155 as maximum cumulative drought severity and maximum duration. However, as no substantial difference  
156 was found (see Supplementary Table S2), we opted for using maximum drought severity as a predictor  
157 for subsequent analyses.

158 In the first panel data model (Eq. 1, 2 and 3), we quantified the relationship between the variability of  
159 streamflow-to-precipitation and maximum drought severity for meteorological, soil moisture,  
160 hydrological droughts and NDVI anomalies. We considered the full length of the available timeseries  
161 (1982 to 2016) and the influence of drought severity in the same year and the year after (i.e.,  $t$  and  $t-1$   
162 in Equation 1). Drought type variables included in the model formulation were selected based on



correlation analysis (Figure S1 in Supplementary Information) and the length of their timeseries. For  
 soil moisture drought, we used the maximum anomaly severity between soil moisture surface and root,  
 165 given the high correlation between these anomalies (Figure S1c). Hydrological drought combining  
 streamflow, surface water extent, and total water storage was chosen over the individual variables, as  
 the latter two overlap with the other variables only for the last 10 years of data. Thus, hydrological  
 168 drought was computed as the maximum anomaly severity among streamflow, surface water extent, and  
 total water storage.

$$171 \quad \left(\frac{Q}{P}\right)_{ct} = (\alpha + \alpha_c) + \sum_i^p (\beta_i + \beta_{ic}) * D_{i(t)} + \sum_i^p (\gamma_i + \gamma_{ic}) * D_{i(t-1)} + \varepsilon \quad (1)$$

$$\sum_i^p D_{i(t)} = D_{M_{sv}(t)} + D_{SM_{sv}(t)} + D_{HY_{sv}(t)} + D_{NDVI_{sv}(t)} \quad (2)$$

$$\sum_i^p D_{i(t-1)} = D_{M_{sv}(t-1)} + D_{SM_{sv}(t-1)} + D_{HY_{sv}(t-1)} + D_{NDVI_{sv}(t-1)} \quad (3)$$

174

Where:

$c$  is a catchment index and  $t$  is for year;

177  $\left(\frac{Q}{P}\right)_{ct}$ : Ratio between annual average streamflow [mm/d] and precipitation [mm/d] calculated for the  
 year  $t$  in catchment  $c$ ;

$\alpha$ : Intercept ( $\alpha$  for the fixed effect and  $\alpha_c$  for the catchment specific effect);

180  $D_{i(t)}$ : Max drought severity in the year  $t$  (M: meteorological; SM: soil moisture, HY: hydrological and  
 NDVI anomalies);

$D_{i(t-1)}$ : Max drought severity ( $sv$ ) in the previous year (M: meteorological; SM: soil moisture, HY:  
 183 hydrological and NDVI anomalies);

$\beta_i$ : Unique effect of drought  $i$  occurred in time  $t$  on the streamflow-to-precipitation ratio;

$\beta_{ic}$ : Unique effect of drought  $i$  occurred in time  $t$  on the streamflow-to-precipitation ratio for  
 186 catchment  $c$ ;

$\gamma_i$ : Unique effect of drought  $i$  occurred in time  $t-1$  on the streamflow-to-precipitation ratio;

$\gamma_{ic}$ : Unique effect of drought  $i$  occurred in time  $t-1$  on the streamflow-to-precipitation ratio for  
 189 catchment  $c$ ;

$\varepsilon$ : Error term.



192 In the second panel data model (Eq. 4, 5), we quantified the same relationship but this time using all  
variables as predictors (meteorological, soil moisture, streamflow, surface water extent and total water  
195 storage and NDVI anomalies), starting from 2002 to encompass the last 14 years. This time span was  
chosen to ensure complete overlap of the total water storage and surface water extent timeseries with  
the other variables analysed.

$$198 \quad \left(\frac{Q}{P}\right)_{ct} = (\alpha + \alpha_c) + \sum_z^p (\beta_z + \beta_{zc}) * D_{z(t)} + \varepsilon \quad (4)$$

$$\sum_z^p D_{z(t)} = D_{M_{sv}(t)} + D_{SM_{sv}(t)} + D_{STR_{sv}(t)} + D_{SW_{sv}(t)} + D_{TWS_{sv}(t)} + D_{NDVI_{sv}(t)} \quad (5)$$

201 Where:

$c$  is a catchment index and  $t$  is for year;

$\left(\frac{Q}{P}\right)_{tc}$ : ratio between mean streamflow [mm/d] and precipitation [mm/d] calculated for the year  $t$  in

204 catchment  $c$ ;

$\alpha$ : Intercept ( $\alpha$  for the fixed effect and  $\alpha_c$  for the catchment specific effect);

$D_{i(t)}$ : Max drought severity in the year  $t$  (M: meteorological; SM: soil moisture; STR: streamflow; SW:

207 surface water extent; TWS: total water storage and NDVI anomalies);

$\beta_z$ : Unique effect of drought  $z$  occurred in time  $t$  on the streamflow-to-precipitation ratio;

$\beta_{zc}$ : Unique effect of drought  $z$  occurred in time  $t$  on the streamflow-to-precipitation ratio for

210 catchment  $c$ ;

$\varepsilon$ : Error term.

213 We assessed possible correlations among the predictors using Pearson correlation analysis. In the first  
model, the highest correlation (0.16) is observed between soil moisture and hydrological drought (Figure  
S1-e in Supplementary Information). In the second model, the highest correlation (0.18) is found  
216 between streamflow drought and soil moisture (Figure S1-d in Supplementary Information). Similar  
correlation values were obtained using Spearman correlation analysis, which accounts for non-linear  
relationships (Figure S2 in Supplementary Information). These correlations are assumed to not  
219 significantly influence the estimation of the coefficients.

Autocorrelation in the residuals leads to an incorrect estimation of the variance of the estimated  
regression coefficients, hence a possible overestimation of the test significance (Anderson 1954).



222 Therefore, we applied the Durbin-Watson test (Bartels and Goodhew 1981) to check for possible  
autocorrelation between the residuals, obtaining values between 1 and 2, indicating little to no  
autocorrelation. We also applied the fixed effects panel data model with clustered standard errors  
225 (Moody, 2017) by catchment to test the robustness of our results. By using clustered standard errors, we  
allow for the possibility of correlated errors within each catchment, while assuming that errors are  
independent across different catchments. As the number of clusters grows, the cluster-robust standard  
228 errors become consistent. In applying the fixed-effects panel data model, we used the same regressions  
as in Equation 1 and 4. We first constructed a panel model using all available catchments, which yielded  
results consistent with those of the mixed-effects panel data model. Subsequently, we grouped  
231 catchments according to climate types - such as arid, snow, warm temperate, and equatorial, aligning  
with the Köppen-Geiger climate classification (Rubel and Kottek, 2010) and we applied the model to  
each category. Finally, we categorized the catchments according to climate and soil types, as well as  
234 climate and land cover types. For the soil-based categorization, we utilized soil classifications derived  
from the fractions of sand, silt, and clay within each analysed catchment, as provided by the GSIM  
dataset (Do et al. 2018; Gudmundsson et al. 2018). The land cover types used in the second  
237 categorization - 'Forest', 'Shrubland', 'Grassland' and 'Agriculture' - were also sourced from the GSIM  
dataset, which uses the United Nation Classification System for 2015 (European Space Agency (ESA)  
2017) and assigns the land cover type that occupies more than 50% of the catchment area. The  
240 application of the fixed-effects panel data model to different clusters allowed us to compare coefficients  
across various catchment characteristics, and analyse whether these characteristics might alter the  
drought influence on the Q-P relationship.

243 The coefficients associated with the independent variables are dimensionless and indicate the magnitude  
of change in the sensitivity of streamflow to precipitation for a one-standard change in each respective  
independent variable, while holding all other variables constant. Finally, we analysed the spread of these  
246 coefficient values with catchment characteristics: mean annual catchment precipitation, maximum  
altitude, population density, and artificial water storage. The mean annual precipitation was computed  
using precipitation time series extracted from the MSWEP dataset, while the other variables were  
249 obtained from the GSIM dataset (Do et al. 2018), which provides various attributes of catchment  
characteristics.

#### 252 **2.4 Trend and step-change analysis for non-stationary Q-P timeseries**

To identify shifts in the streamflow response to precipitation from one steady state to another, we carried  
out a trend analysis in 1107 catchments with non-stationary streamflow-to-precipitation (Q-P) ratio  
255 timeseries. This involved modelling the relationship between the Q-P ratio and year (adapting the  
methodology in Berdugo et al. 2022). In detail, we investigated whether the Q-P trends are linear (i.e.,  
monotonic trends or no trends), curvilinear (with an acceleration or deceleration that makes the trend





258 nonlinear), or abrupt (characterized by a sudden change maintained until the end of the time period  
under analysis). We applied linear and quadratic models to test for linearity and nonlinearity,  
respectively, and also assessed the fit without a trend. Additionally, we used a threshold regression  
261 approach to detect any abrupt changes in the Q-P relationship. This approach models the relationship  
between variables that change at a specific threshold (i.e., change point). When multiple state transitions  
occurred within the analysed period, the method identifies the candidate change point that maximizes  
264 the goodness-of-fit or minimizes the loss function.

To select the best fitted model for each trend, we compared the Akaike Information Criteria (AIC;  
Wagenmakers and Farrell 2004) values of each fit. AIC is based on the log-likelihood of a given fit. A  
267 lower value indicates a model that fits the data better, but candidates with AIC differences lower than  
two units usually are similarly good.

To account for potential uncertainty in classifying trends due to their noisy nature and the relatively  
270 short length of the timeseries, we bootstrapped each timeseries 100 times without replacement and  
compared the model results of each bootstrapped iteration. For each bootstrap, we increased the  
probability of selecting the least influential points using the distance-based Mahalanobis method  
273 (Berdugo et al. 2022; Liu et al. 2018). We then computed the number of times that each model was  
selected as best-fit out of the 100 bootstraps, to identify the best fitted shape for each trajectory. We used  
this percentage as a measure of confidence for the best-fit shape of each trajectory (hereafter called  
276 confidence value).

Given the sensitivity of step regressions to outliers, we implemented three criteria to increase confidence  
in detecting step trends. First, we discarded step trends where the change point fell within the first or  
279 last three years of the period of analysis. This ensured that abrupt changes were not falsely identified  
due to anomalous data points at the start and end of the timeseries and guaranteed that detected abrupt  
changes persisted for at least four years after the change, indicating a certain stability of the change  
282 detected.

Second, we recorded the change point position (i.e., the year in which the trend is detected to change  
abruptly) for each trajectory classified as ‘step-change’ and calculated the mean and standard deviation  
285 (SD) of these change points across the 100 bootstrap iterations of each catchment. To determine the  
value of the change point SD that is critically influencing anomalous steps, we related the confidence  
value in the bootstrap selection and the SD of change points in all sites. We found that both parameters  
288 were related: for Q-P ratio timeseries in which the SD of change point was lower than 6 years, there was  
a strong negative correlation between the SD of change point and the confidence value in the bootstrap  
selection, whereas higher SDs in change point showed similarly low confidence values (Figure S3 In  
291 Supplementary Information). Therefore, we only considered step changes with standard deviations  
below 6 and confidence values above 80%.



294 Third, we categorized trajectories as step-change only if the Q-P ratios before and after the change point  
significantly differed according to a two-sample Kolmogorov-Smirnov test. This criterion ensured that  
the observed change point was sufficiently robust, aligning with the definition of a regime shift,  
characterized by significant differences in functioning or structure between two states. The analysis was  
297 carried out with a significance level of 0.05. For each of the trajectories classified as step-change, we  
identified the direction of the step as positive (increasing trend) or negative (decreasing trend). We then  
continued our analysis only considering the catchments with a step change in the Q-P timeseries.

300 For the trends classified as ‘step-change’, we examined drought anomalies occurring during and before  
the identified change years. Drought severity was categorized as moderate (between the 15th and 10th  
percentiles), severe (between the 10th and 5th percentiles), and extremely severe (below the 5th  
303 percentile).

### 3. Results

#### 3.1 Drought influence on streamflow sensitivity to precipitation for stationary catchments

306 Generally, droughts tend to decrease the sensitivity of streamflow to precipitation (negative coefficient  
values in Figure 2a and Tables S2 to S4), with hydrological drought having a more pronounced effect  
compared to other drought types. Soil moisture drought is the second most predominant factor (Figure  
309 2a). In contrast, negative NDVI anomalies exhibit a slight increase (3%) in streamflow sensitivity to  
precipitation. The influence of drought persists into the following year, maintaining the same direction  
(in terms of increased or decreased sensitivity to different drought types) but with a reduced magnitude.

312 Further, both drought severity and duration show a similar influence on streamflow sensitivity to  
precipitation (Table S2), likely due to the moderate correlation between these two variables.

While on average we find reduced streamflow sensitivity to precipitation during drought events, spatial  
315 variations among catchments exist (Figure 2b and Figure 3). In most climate zones, hydrological drought  
has the strongest influence on the Q-P relationship (Figure 2b). Arid regions are an exception, with soil  
moisture drought having the strongest influence on the Q-P relationship (a one-standard deviation  
318 increase in soil moisture drought severity leads to a 30% decrease in the Q-P ratio; Figure 2b). Further,  
NDVI anomalies in arid regions lead to a decrease in sensitivity (a one-standard deviation increase in  
NDVI anomalies leads to a 3% decrease in the Q-P ratio) compared to the slight increase (around 5%)  
321 in sensitivity found in the other climate regions. Catchments located mainly in polar, snow-influenced  
and equatorial regions present the lower coefficient values, indicating less changes in streamflow  
sensitivity to precipitation during drought events (Figure 2b and Table S5). These findings are further  
324 supported by the random effects model, which identifies catchments with lower coefficient values in the  
Apennine region, southwest Canada, northeast United States, and central Brazil (Figure 3 and Figure S4  
of the Supplementary Information).

327

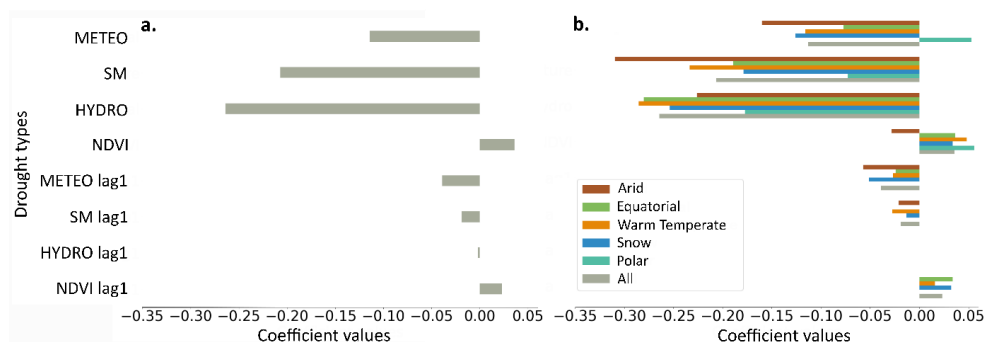


**Figure 2.** Bar plots of the panel data models' coefficient values for each drought type variable (METEO: meteorological, SM: soil moisture, HYDRO: hydrological and NDVI anomalies) with and without a lag time of 1 year. (a) Fixed effect coefficients from the mixed-effects panel data model. (b) Fixed effect coefficients from the panel data model with clustered standard errors, including all data and data grouped by climate types (refer to Table S4). All results are significant with  $p$ -values  $< 0.001$ , while results marked with asterisks indicate levels of significance: \*  $p < 0.1$  and \*\*  $p < 0.01$ . Missing bars indicate coefficients with  $p$ -values  $> 0.1$ , which are reported as NaN.

336

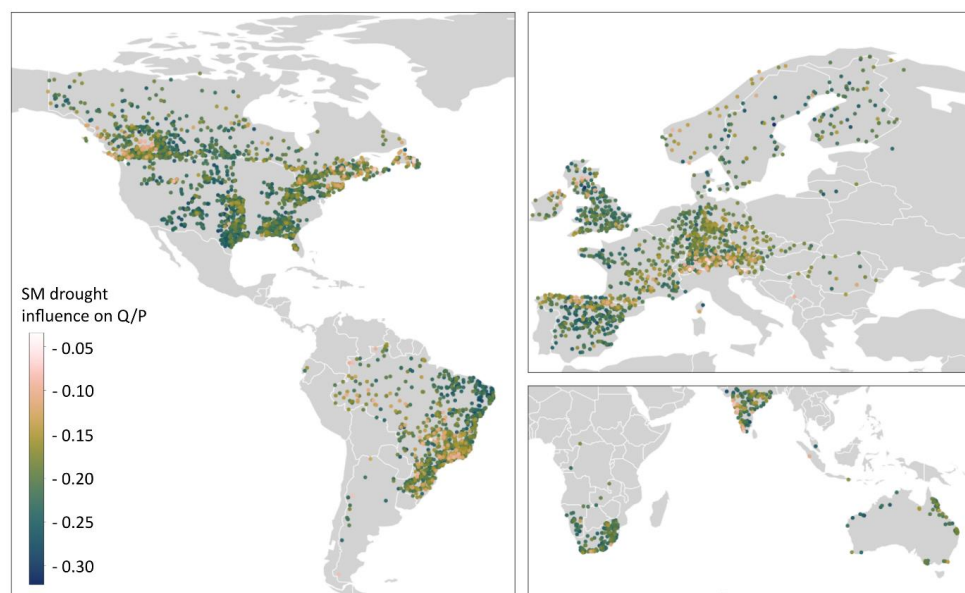


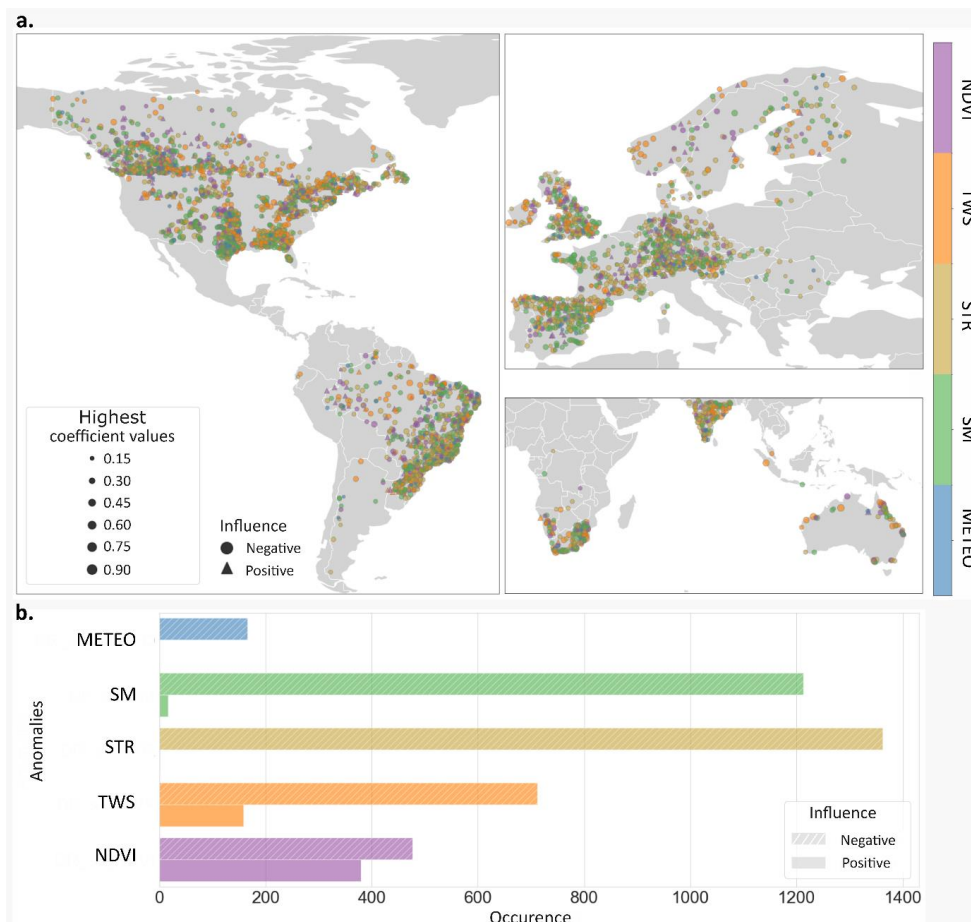
**Figure 3.** Catchment-specific effects of soil moisture (SM) drought on the Q-P ratio captured with the mixed-effects panel data model. Results are shown only for soil moisture as it exhibits the largest spatial variation compared to other drought types, which are reported in Supplementary Figure S3.

By identifying the dominant drought type, indicated by the highest regression coefficient value in each catchment, we determined which drought type primarily influences the Q-P relationship spatially

342



(Figure 4a). This analysis also allowed us to assess the degree of catchment resilience to Q-P changes during droughts. Hydrological and soil moisture drought emerge as the most influential drought type (respectively for 30 and 27% of the catchments and indicated in brown and green in Figure 4), predominantly dampening the sensitivity of Q to P (Figure 4b). Soil moisture drought dominates in catchments clustered in the southcentral United States, southern Spain, and northeast India. On the other hand, anomalies in total water storage and NDVI affect Q-P relationships in 19% of the catchments each, with total water storage anomalies mainly in snow-influenced regions and northern Australia. Catchments with the highest regression coefficients (absolute values above 0.7) and indicating the lowest resilience to drought influence on Q-P relationships, are located in north Australia and the south-central/eastern United States and are primarily influenced by soil moisture and groundwater drought. The most resilient catchments (absolute coefficient values below 0.2) are found in the Alpine region and in southeast Brazil.





357 **Figure 4.** Highest regression coefficient per catchment, indicating the predominant drought type (among  
meteorological (METEO), soil moisture (SM), streamflow (STR), total water storage (TWS), and NDVI)  
360 influencing streamflow sensitivity to precipitation, as determined by the mixed-effects panel data model with time  
series data spanning the last 14 years (starting from 2002) and using Equation 2. This timeframe enables a full  
overlap of GRACE data with other variables. Coefficients of drought anomalies in surface water extent were  
363 excluded from the analysis due to nonsignificant results ( $p > 0.1$ ). (a) Spatial distribution of the predominant  
drought type per catchment. Marker size corresponds to the magnitude of the highest coefficient. Circular markers  
represent a decrease in sensitivity of streamflow to precipitation, while triangle markers indicate an increase in  
366 sensitivity. (b) Fraction of catchments with positive and negative coefficients of the predominant drought type per  
climate zone.

Spatial variations in streamflow sensitivity to precipitation due to drought are influenced by both  
topography and climate characteristics, but to different degrees. Altitude variation has a minimal effect  
369 on the influence of drought on streamflow sensitivity to precipitation (Figure S5 in Supplementary  
Information). As maximum catchment altitude increases, the sensitivity of catchment response to  
meteorological and soil moisture drought slightly decreases across all climate regions except arid ones,  
372 with this effect being particularly noticeable in the Alps, Pyrenees, mountain ranges of Norway, and the  
Canadian coastal mountains. In contrast, mean catchment precipitation exhibits a more pronounced  
effect, with a decrease in the drought influence on the Q-P ratio as mean catchment precipitation  
375 increases (Figure S6 in Supplementary Information). The exception to this is hydrological drought,  
whose influence on streamflow sensitivity to precipitation slightly increases when mean catchment  
precipitation increases.

378 While climate types primarily influence variations in drought impacts on Q-P relationships across  
catchments, predominant land cover also plays a significant role (Supplementary Figure S8).  
Catchments dominated by grasslands and shrublands are more sensitive to Q-P changes induced by soil  
381 moisture drought, whereas those with forests and agricultural areas exhibit greater fluctuations in Q-P  
relationships during hydrological drought (first row of the heatmap in Supplementary Figure S8). These  
differences become more pronounced when catchments are clustered by both climate and land cover  
384 (Supplementary Figure S8). Specifically, grasslands in arid and equatorial regions exhibit heightened  
susceptibility to Q-P changes during drought. In snow-influenced climates, shrublands experience the  
most significant changes, while in warm temperate regions, agricultural and forested areas are the most  
387 affected. Conversely, negative NDVI anomalies have a minimal effect on the Q-P relationship in  
catchments dominated by grasslands.

Clustering catchments based on soil and climate type reveals that those in both snow-influenced regions  
390 and with sandy soils (sand fraction  $>33\%$ ) exhibit the least changes in streamflow sensitivity to  
precipitation due to drought (Supplementary Figure S9). Q-P ratios in arid and equatorial sandy  
catchments are significantly influenced by soil moisture drought, while hydrological drought plays a



393 key role in warm temperate catchments with both clay and sandy soils. By clustering the catchments  
according to the total storage of the dams within a catchment, we can see that the influence of drought  
on the Q-P relationships slightly increases with an increase of reservoir storage (Supplementary Figure  
396 S11).

### 3.2 Analysis of step change in Q-P relationship for non-stationary catchments

399 The step analysis identified 197 catchments with a step change in the Q-P ratio timeseries, 183 of which  
occur during drought conditions. The percentage of catchments showing a step change was similar for  
both undisturbed and human-influenced (presence of reservoirs) catchments, at around 16%. Among the  
402 human-influenced catchments, 70% showed a negative step, whereas the undisturbed catchments were  
nearly evenly split, with about 52% exhibiting a positive step and 48% a negative step.

Catchment clusters with positive steps in the Q-P relationship (i.e., increased sensitivity of streamflow  
405 to precipitation) are primarily found in snow-influenced regions but are also present across other climate  
regions (Figure 5d). Those catchments are concentrated in the north-central United States, western  
Canada, and northeastern Brazil. Conversely, catchment clusters with negative step are found in southern  
408 Canada, scattered across Alpine and Scandinavian countries, and central Brazil. By plotting the years in  
which the steps occurred, we could identify some notable drought events (Figure 5). For instance, a  
cluster of catchments with negative step trend has the step change during the 2011-2012 drought that  
411 severely affected north-east Brazil (Rodrigues and McPhaden 2014). Within this cluster, only one  
catchment exhibits a positive step change. This catchment shares the same equatorial climate and has  
similar land cover as the others in the cluster (Table S6). The only notable difference is its significantly  
414 smaller size (hundreds of square kilometers compared to the others which span thousands).

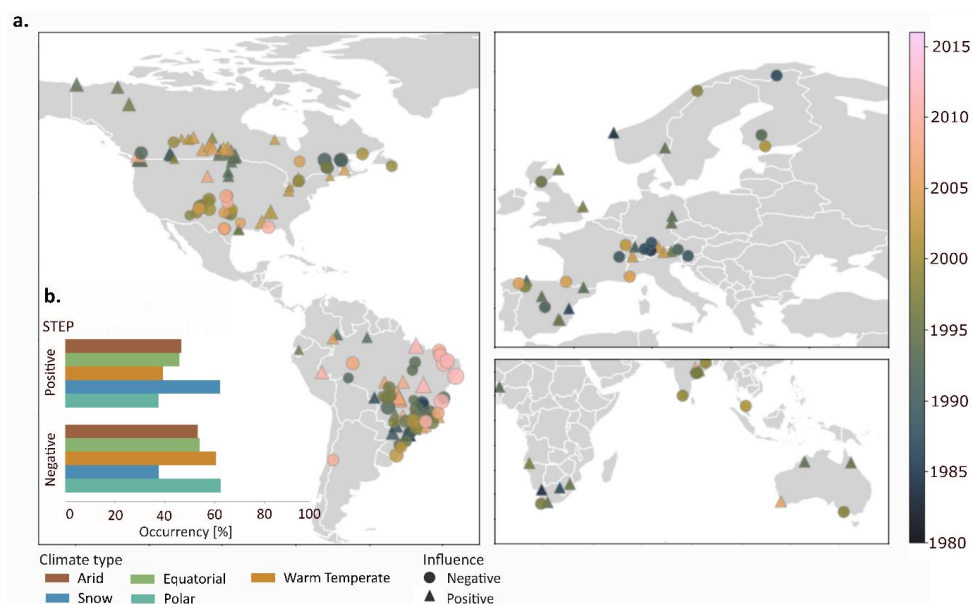


**Figure 5.** Global maps (a) of catchments whose Q-P ratio timeseries presents a step trend with a positive (triangle markers) or negative (circle markers) step. Marker colours indicate the years in which the step change occurred. Marker size indicate the magnitude of the shift. b. Occurrence of positive or negative step change in Q-P relationship across catchments located in Arid, Warm temperature, Equatorial, Snow and Polar climate regions.

417

420

Drought events occurring during shifts in the Q-P relationship are typically extremely severe (below the 5th percentile; Figure 6a and b). This is especially pronounced in meteorological droughts and NDVI anomalies for negative shifts, and in soil moisture droughts for positive shifts. Our analysis of drought preceding the change year reveals longer durations of soil moisture and hydrological drought (>1 year) for positive step trends, and longer durations of NDVI and meteorological droughts for negative steps (>10 months; Figure 6c and Supplementary Figure S13).

423

426

Finally, 96% of drought events detected during the change year had more than one anomaly, with 92% including meteorological droughts. Instances where the drought anomaly was solely meteorological resulted mainly in a decrease in the Q-P ratio following the step change (19% of catchments, Figure 7a). Conversely, instances showing positive shifts were mainly related to at least two components of the hydrological system experiencing drought anomalies (Figure 7b). Specifically, both positive and negative shifts are initiated by precipitation anomalies, but the shift is positive mainly when this anomaly propagates to soil moisture (88% of catchments, Figure 7b) and then to the hydrological system (75% of catchments, Figure 7b).

429

432

435

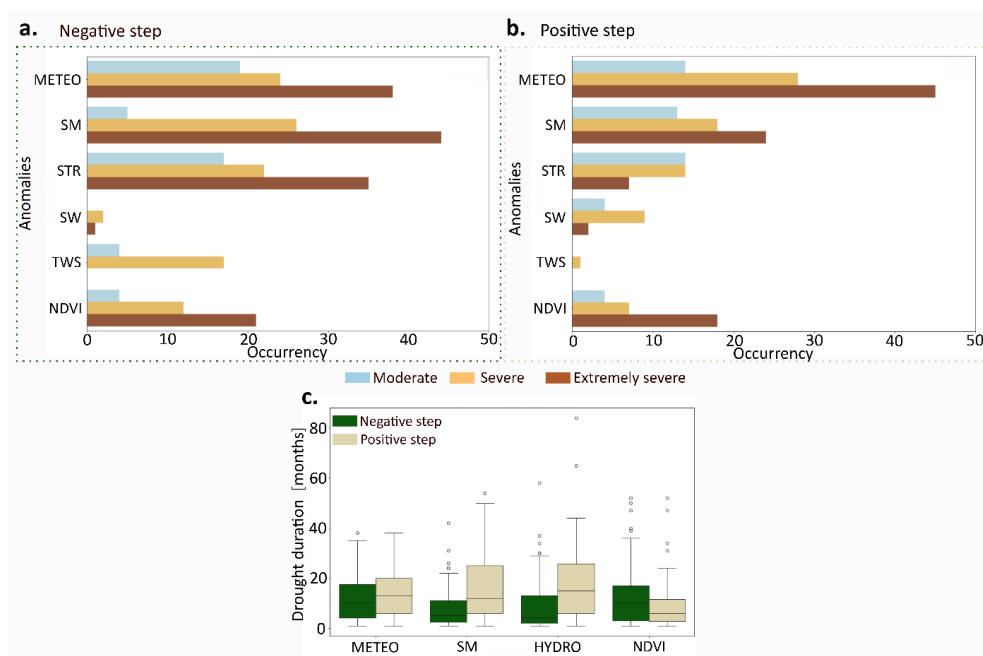
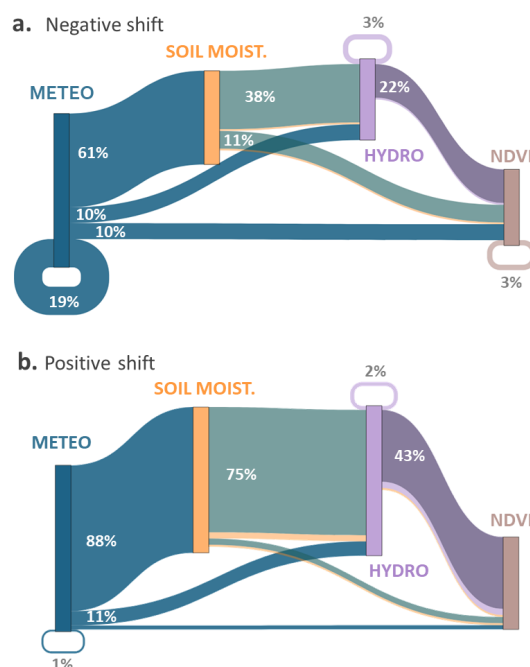


**Figure 6.** Analysis of severity and duration of drought events detected during the change years. (a-b) Occurrences of different drought types (meteorological (METEO), soil moisture (SM), streamflow (STR), surface water extent (SW), total water storage (TWS), and NDVI) for negative (a) and positive (b) steps. The fractions of total occurrences classified as moderate ( $10^{\text{th}} < x < 15^{\text{th}}$ ), severe ( $5^{\text{th}} < x < 10^{\text{th}}$ ), or extremely severe ( $x < 5^{\text{th}}$ ) droughts are represented by blue, yellow, and brown colours, respectively. (c) Total number of months under anomalies of consecutive drought years preceding the change year (drought may persist after the change year).





444

**Figure 7.** Percentage of drought types (co-)occurring during negative (a) and positive (b) shifts, propagating from precipitation, soil moisture, and streamflow droughts to further droughts along the drought propagation pathway.

447

For example, in panel (b), the blue flow leading to the yellow bar (88%) indicates the co-occurrence of meteorological and soil moisture droughts, while the blue flow leading to the brown bar (11%) indicates the co-occurrence of meteorological drought and NDVI anomalies. Flow colours represent the co-occurrence of multiple anomalies (e.g., the green flow (75%) represents the co-occurrence of meteorological, soil moisture, and hydrological droughts). Circular flows (loops returning to the same drought type) represent events where only one anomaly was detected, indicating no further propagation of drought within the system. Percentages are calculated

450

separately for positive and negative steps, representing the proportion of catchments exhibiting each specific co-occurrence relative to the total number of catchments showing a step change.

453

456

## 4. Discussion

### 4.1 Drought influence on Q-P relationship in stationary catchments

459

The panel data analysis showed that drought in general decreases streamflow sensitivity to precipitation in stationary catchments (Figure 2 and Figure 3), aligning with previous research (Liu et al. 2021; Massari et al. 2022; Maurer et al. 2022; Saft, Peel, Western, Perraud, et al. 2016). This tendency can be explained by initial precipitation being used to replenish catchment water storage before streamflow

462

responds (Barendrecht et al. 2024; Van Loon and Laaha 2015; Parry et al. 2016), which is further confirmed by the higher influence of hydrological and soil moisture drought on the Q-P relationship compared to meteorological drought and NDVI (Figure 2). On the other hand, negative NDVI anomalies



465 lead to a slight increase of streamflow sensitivity to precipitation (Figure 2). This increase can be  
attributed to decreased evapotranspiration and reduced water uptake from dying vegetation (Breshears  
et al. 2005; Zhang et al. 2019). In smaller catchments (hundreds of square kilometers), an increase in Q-  
468 P relationship may also be due to drought-induced soil compaction, which leads to reduced infiltration  
and higher runoff (Alaoui et al. 2018; Descroix et al. 2009).

Despite a predominant tendency of decreasing streamflow sensitivity to precipitation during drought,  
471 the severity of this influence and the underlying processes differs spatially. Arid regions, for instance,  
show less resilience to drought, which significantly influences catchment response to precipitation. This  
finding aligns with earlier studies (Liu et al. 2023; Maurer et al. 2022; Saft et al. 2015), which observed  
474 higher susceptibility to change in hydrological behaviour during persistent drought in arid catchments.  
Our study further reveals that Q-P relationship arid regions are particularly sensitive to soil moisture  
drought (Figure 3). This suggests that decreases in subsurface flow, which affect vegetation cover and  
477 surface water-groundwater interactions, are primary mechanisms driving reduced streamflow sensitivity  
to rainfall. Conversely, snow-influenced and polar regions are more resilient to drought-induced changes  
in the Q-P relationship (Figure 2b) due to their high storage capacity. In these basins, snowmelt during  
480 drought can replenish subsurface storage, compensating for reduced precipitation inputs and limiting  
the dependency of evapotranspiration on deep subsurface storage (Avanzi et al. 2020). In these regions,  
the relationship between precipitation and streamflow is strongly influenced by drought anomalies in  
483 the total water storage (Figure 4), as confirmed by (Berghuijs and Slater 2023; Carroll et al. 2024; van  
Tiel et al. 2024), who highlight the importance of groundwater for mountain streamflow.

Spatial differences can also be found in the influence of negative NDVI anomalies on the Q-P  
486 relationship. While the sensitivity of the Q-P relationship generally increases during negative NDVI  
anomalies, in arid and semi-arid catchments, this sensitivity decreases (Figure 2b). This decrease could  
be explained by reduced connectivity among bare patches (Urgeghe et al. 2010) and increased soil  
489 evaporation due to an increase in solar radiation reaching the ground (Guardiola-Claramonte et al. 2011).

Spatial variations are also driven by topographic characteristics and landcover type, although climate  
characteristics appear to be more predominant. In general, soil moisture and meteorological drought  
492 have a slightly smaller influence on streamflow sensitivity to precipitation at higher altitudes, with this  
behaviour accentuated mainly in certain areas such as the Alps and Pyrenees. The same effect was found  
by Maurer et al. (2022) and explained by the resilience of high-elevation runoff to increases in potential  
495 evapotranspiration due to overall lower temperatures and sparser vegetation (Garreaud et al. 2017),  
which help mitigate runoff losses elsewhere in the basin. By analysing land cover, we find that forests  
reduce the influence of meteorological drought on catchment response, likely due to their higher  
498 hydraulic diversity, which buffers precipitation anomalies (Anderegg et al. 2018). However, when  
drought affects the hydrological system, forests present marked changes in catchment response. A



501 similar effect is observed in agricultural and grassland catchments, but specifically in response to soil  
moisture drought.

504 While the impact of human influence (i.e., reservoirs) on drought-induced changes on the Q-P  
relationship is relatively weak, average catchment wetness—represented by mean annual  
precipitation—appears to have a stronger influence. In detail, we found a substantial decrease of soil  
moisture drought influence on the Q-P relationship with an increase in wetness which could be explained  
by the buffering effects of water storage (Liu et al. 2022).

507

#### 4.2 Q-P shifts during drought in non-stationary catchments

510 The analysis of step changes in the Q-P relationship in non-stationary catchments showed slightly  
different patterns in how streamflow sensitivity to precipitation shifts during drought conditions,  
compared to Q-P fluctuations during drought in stationary catchments. While the study of drought  
513 influence primarily indicated a drought-induced decrease in streamflow sensitivity to precipitation, the  
step-change analysis identified both positive and negative shifts (Figure 5). These shifts occurred in  
various climate regions and under different catchment characteristics. This suggests that catchments  
516 might experience changes in the rainfall-runoff relationship regardless of their predominant climate and  
catchment characteristics.

519 Although both positive and negative Q-P shifts are found in catchments in different climate regions,  
catchments in snow-influenced regions exhibited a slight tendency toward positive shifts. These  
consistent increases in streamflow sensitivity to precipitation for at least four years after the shift can be  
explained by permafrost thaw (Lamontagne-Hallé et al. 2018) and glacial melt (Fountain and Tangborn  
522 1985; Lutz et al. 2014; Schaner et al. 2012). While these mechanisms can sustain increased streamflow  
sensitivity to precipitation, they are ultimately finite resources. As glaciers and permafrost deplete and  
precipitation increasingly falls as rain, streamflow will eventually reduce (Berghuijs, Woods, and  
525 Hrachowitz 2014).

528 Contrary to the drought influence on stationary Q-P relationships, the severity and duration of droughts  
play a critical role in shaping these step changes (Figure 6). Our analysis indicates that severe droughts  
especially with longer durations are often linked to positive step changes in the Q-P relationship. For  
instance, positive step changes are frequently preceded by extended periods of severe soil moisture and  
hydrological drought, reflecting how persistent drought anomalies in the hydrological system can lead  
531 to significant adjustments in catchment response. These adjustments can be related to drought-induced  
changes in soil hydraulic properties (Alaoui et al. 2018; Descroix et al. 2009), vegetation type (Adams  
et al. 2012), interaction between shallow groundwater tables and soil moisture (Barendrecht et al. 2024).  
534 Conversely, negative step changes can occur after shorter drought periods, often linked to  
meteorological droughts. This suggests that negative step changes might be associated with more abrupt



537 climatic shifts rather than longer-term changes in hydrological processes. This is further confirmed by  
the observation that positive Q-P shifts occur only when anomalies propagate through the hydrological  
system, resulting in multiple detected anomalies. In contrast, negative shifts can be recorded with only  
a decline in rainfall (Figure 7).

540 While there are no significant differences between catchments with human influence and those that are  
undisturbed when analysing drought influence on Q-P fluctuations, more pronounced differences  
emerged when analysing Q-P shifts during drought. Shifts occur in both catchments with reservoirs and  
543 those that are undisturbed. However, negative shifts are prevalent in catchments with reservoirs. This  
trend may be attributed to changes in reservoir operational rules aimed at drought mitigation (Di  
Baldassarre et al. 2017). Since a shift in our analysis must persist for at least four years to be considered  
546 significant, this suggests that drought events have a lasting impact on reservoir operational strategies.  
These findings indicate that drought not only alters the Q-P relationships due to changes in the  
hydrological system but also through changes in risk perception and adaptation responses.

549

#### 4.3 Limitations and challenges

The methodology and data employed in this study comes with a few limitations and challenges.

552 Firstly, the precision of estimates in mixed-effects panel data models improves with longer time series,  
as they enable more accurate modelling of random effects and mitigate the influence of short-term noise.  
Similarly, trend analysis benefits from extended time series. However, increasing the length of the time  
555 series can reduce spatial coverage by excluding some catchments. To balance long-term coverage with  
spatial representation, we opted for a minimum time span of 25 years for streamflow and precipitation  
data. This decision, coupled with strict data quality checks (detailed in Matanó et al., 2024), resulted in  
558 underrepresentation of regions such as Asia, Australia, northern and central Africa, and the western  
United States in our analysis.

Another significant challenge was the absence of GRACE measurements before 2002, which resulted  
561 in missing total water storage (TWS) anomalies for earlier years. Additionally, the surface water extent  
time series began in 1984, three years later than other variables. This led to a trade-off between  
maximizing the length of the time series in the panel data model and ensuring full overlap of all  
564 variables. To address this, we computed a new variable, the hydrological anomaly, summarising the  
anomalies in streamflow, surface water extent, and TWS to ensure a consistent time span with the other  
variables. Additionally, we ran the panel data models using the last 18 years of data to guarantee full  
567 overlap of the variables without aggregation.

Finally, another challenge lies in bridging the 'scale gap' between drought events, which occur on an  
event time scale, and the streamflow-precipitation ratios, which are computed on an annual time scale.



570 To mitigate this, we calculated various metrics to represent the characteristics of drought events on a  
yearly basis, attempting to reconcile these different temporal scales within our analysis.

## 573 **5. Conclusion**

This study used panel data models to examine the effects of drought type, duration, and severity on  
streamflow sensitivity to precipitation, accounting for variations in climate types, altitudes, land cover  
576 and average precipitation levels. Our analysis generally revealed a decrease in streamflow sensitivity  
during droughts in stationary catchments, except in cases of negative NDVI anomalies, which slightly  
increased sensitivity. Spatial variability was evident, with arid and semi-arid regions showing lower  
579 resilience to drought-induced changes in the Q-P relationship, while wet catchments, such as those in  
snow-influenced climates, showed greater resilience due to their water-buffering mechanisms. This  
trend of reduced sensitivity intensified with longer and more severe droughts, though the effects of  
582 duration and severity were similar in magnitude. Further analyses based on step-change methods in non-  
stationary catchments revealed both positive and negative shifts in sensitivity. Specifically, longer and  
more severe droughts related to soil moisture and hydrology often resulted in positive shifts in  
585 sensitivity, whereas shorter, more abrupt meteorological droughts were associated with negative shifts.  
These findings underscore the complexity of drought impacts on the Q-P relationship and highlight the  
importance of considering both drought characteristics and regional differences when evaluating  
588 streamflow responses. Understanding these sensitivities is crucial for assessing the resilience and  
adaptability of catchments to drought, given its distinct roles in influencing flow regimes.

## 591 **Data and code availability**

All data used in this study come from secondary datasets which are publicly available at the time of  
publication. Data regarding streamflow data are available through the GSIM dataset at  
594 <https://doi.pangaea.de/10.1594/PANGAEA.887477> (Do et al. 2018; Gudmundsson et al. 2018).  
Precipitation data can be downloaded at <https://www.gloh2o.org/mswep/> (Beck et al. 2019b). Data on  
drought events are openly available at the following URL/DOI:  
597 <https://figshare.com/s/a06830fc5111bd7804ce> (Matanó et al 2023). Python and R code for the complete  
analysis are available at <https://figshare.com/s/20227bda9e89aca586da>.

600 **Author contributions.** The conceptualization and methodology were designed by AM, AFVL, RH,  
MIB and MHB. Data curation, formal analysis, investigation, software handling, visualization, and  
writing (original draft preparation) were performed by AM. Supervision and validation were carried out  
603 by AFVL, RH, MIB and MHB. Writing (review and editing) was carried out by AFVL, RH, MIB, MHB  
and AM.



606 **Competing interests**

One of the (co-)authors is a member of the editorial board of HESS.

609 **Acknowledgements**

This research was funded by the European Union (ERC, PerfectSTORM, ERC-2020-StG 948601). Views and opinions expressed are however those of the authors only and do not necessarily reflect those of the European Union or the European Research Council Executive Agency. Neither the European Union nor the granting authority can be held responsible for them. The authors thank SURF ([www.surf.nl](http://www.surf.nl)) for the support in using the National Supercomputer Snellius. RH acknowledge funding from the European Union's Horizon 2020 research and innovation programme under Grant Agreement No. 101003469 (XAIDA). MIB acknowledges funding by the Swiss National Science foundation (project 200021\_214907).

618

621

624

627

630

633

636



639 **References**

- Adams, Henry D., Charles H. Luce, David D. Breshears, Craig D. Allen, Markus Weiler, V. Cody Hale, Alistair M. S. Smith, and Travis E. Huxman. 2012. "Ecohydrological Consequences of Drought- and Infestation- Triggered Tree Die-off: Insights and Hypotheses." *Ecohydrology* 5(2). doi: 10.1002/eco.233.
- Alaoui, Abdallah, Magdalena Rogger, Stephan Peth, and Günter Blöschl. 2018. "Does Soil Compaction Increase Floods? A Review." *Journal of Hydrology* 557.
- Alvarez-Garreton, Camila, Juan Pablo Boisier, René Garreaud, Jan Seibert, and Marc Vis. 2021. "Progressive Water Deficits during Multiyear Droughts in Basins with Long Hydrological Memory in Chile." *Hydrology and Earth System Sciences* 25(1). doi: 10.5194/hess-25-429-2021.
- Anderegg, William R. L., Alexandra G. Konings, Anna T. Trugman, Kailiang Yu, David R. Bowling, Robert Gabbitas, Daniel S. Karp, Stephen Pacala, John S. Sperry, Benjamin N. Sulman, and Nicole Zenes. 2018. "Hydraulic Diversity of Forests Regulates Ecosystem Resilience during Drought." *Nature* 561(7724). doi: 10.1038/s41586-018-0539-7.
- Anderson, R. L. 1954. "The Problem of Autocorrelation in Regression Analysis." *Journal of the American Statistical Association* 49(265). doi: 10.1080/01621459.1954.10501219.
- Avanzi, Francesco, Joseph Rungee, Tessa Maurer, Roger Bales, Qin Ma, Steven Glaser, and Martha Conklin. 2020. "Climate Elasticity of Evapotranspiration Shifts the Water Balance of Mediterranean Climates during Multi-Year Droughts." *Hydrology and Earth System Sciences* 24(9). doi: 10.5194/hess-24-4317-2020.
- Di Baldassarre, Giuliano, Fabian Martinez, Zahra Kalantari, and Alberto Viglione. 2017. "Drought and Flood in the Anthropocene: Feedback Mechanisms in Reservoir Operation." *Earth System Dynamics* 8(1). doi: 10.5194/esd-8-225-2017.
- Bales, Roger C., Michael L. Goulden, Carolyn T. Hunsaker, Martha H. Conklin, Peter C. Hartsough, Anthony T. O'Geen, Jan W. Hopmans, and Mohammad Safeeq. 2018. "Mechanisms Controlling the Impact of Multi-Year Drought on Mountain Hydrology." *Scientific Reports* 8(1). doi: 10.1038/s41598-017-19007-0.
- Barendrecht, Marlies H., Alessia Matanó, Heidi Mendoza, Ruben Weesie, Melanie Rohse, Johanna Koehler, Marleen de Ruiter, Margaret Garcia, Maurizio Mazzoleni, Jeroen C. J. H. Aerts, Philip J. Ward, Giuliano Di Baldassarre, Rosie Day, and Anne F. Van Loon. 2024. "Exploring Drought-to-Flood Interactions and Dynamics: A Global Case Review." *Wiley Interdisciplinary Reviews: Water*.
- Bartels, Robert, and John Goodhew. 1981. "The Robustness of the Durbin-Watson Test." *The Review of Economics and Statistics* 63(1). doi: 10.2307/1924228.
- Beck, Hylke E., Eric F. Wood, Ming Pan, Colby K. Fisher, Diego G. Miralles, Albert I. J. M. Van Dijk, Tim R. McVicar, and Robert F. Adler. 2019a. "MSWep v2 Global 3-Hourly 0.1° Precipitation: Methodology and Quantitative Assessment." *Bulletin of the American Meteorological Society* 100(3). doi: 10.1175/BAMS-D-17-0138.1.
- Beck, Hylke E., Eric F. Wood, Ming Pan, Colby K. Fisher, Diego G. Miralles, Albert I. J. M. Van Dijk, Tim R. McVicar, and Robert F. Adler. 2019b. "MSWep v2 Global 3-Hourly 0.1° Precipitation:



- 678 Methodology and Quantitative Assessment.” *Bulletin of the American Meteorological Society*  
100(3). doi: 10.1175/BAMS-D-17-0138.1.
- 681 Berdugo, Miguel, Juan J. Gaitan, Manuel Delgado-Baquerizo, Thomas W. Crowther, and Vasilis Dakos.  
2022. “Prevalence and Drivers of Abrupt Vegetation Shifts in Global Drylands.” *Proceedings of  
the National Academy of Sciences of the United States of America* 119(43). doi:  
10.1073/pnas.2123393119.
- 684 Berghuijs, W. R., R. A. Woods, and M. Hrachowitz. 2014. “A Precipitation Shift from Snow towards  
Rain Leads to a Decrease in Streamflow.” *Nature Climate Change* 4(7). doi:  
10.1038/nclimate2246.
- 687 Berghuijs, Wouter R., and Louise J. Slater. 2023. “Groundwater Shapes North American River Floods.”  
*Environmental Research Letters* 18(3). doi: 10.1088/1748-9326/acbecc.
- 690 Boergens, Eva, Henryk Dobslaw, and Robert Dill. 2019. “GFZ GravIS RL06 Continental Water Storage  
Anomalies. V. 0004. GFZ Data Services.”
- 693 Breshears, David D., Neil S. Cobb, Paul M. Rich, Kevin P. Price, Craig D. Allen, Randy G. Balice, William  
H. Romme, Jude H. Kastens, M. Lisa Floyd, Jayne Belnap, Jesse J. Anderson, Orrin B. Myers, and  
Clifton W. Meyer. 2005. “Regional Vegetation Die-off in Response to Global-Change-Type  
Drought.” *Proceedings of the National Academy of Sciences of the United States of America*  
102(42). doi: 10.1073/pnas.0505734102.
- 696 Carroll, Rosemary W. H., Richard G. Niswonger, Craig Ulrich, Charuleka Varadharajan, Erica R. Siirila-  
Woodburn, and Kenneth H. Williams. 2024. “Declining Groundwater Storage Expected to  
Amplify Mountain Streamflow Reductions in a Warmer World.” *Nature Water* 2(5):419–33. doi:  
699 10.1038/s44221-024-00239-0.
- 702 Descroix, L., G. Mahé, T. Lebel, G. Favreau, S. Galle, E. Gautier, J. C. Olivry, J. Albergel, O. Amogu, B.  
Cappelaere, R. Dessouassi, A. Diedhiou, E. Le Breton, I. Mamadou, and D. Sighomnou. 2009.  
“Spatio-Temporal Variability of Hydrological Regimes around the Boundaries between Sahelian  
and Sudanian Areas of West Africa: A Synthesis.” *Journal of Hydrology* 375(1–2). doi:  
10.1016/j.jhydrol.2008.12.012.
- 705 Do, Hong Xuan, Lukas Gudmundsson, Michael Leonard, and Seth Westra. 2018. “The Global  
Streamflow Indices and Metadata Archive (GSIM)-Part 1: The Production of a Daily Streamflow  
Archive and Metadata.” *Earth System Science Data* 10(2). doi: 10.5194/essd-10-765-2018.
- 708 Donchyts, Gennadii, Fedor Baart, Hessel Winsemius, Noel Gorelick, Jaap Kwadijk, and Nick Van De  
Giesen. 2016. “Earth’s Surface Water Change over the Past 30 Years.” *Nature Climate Change*  
6(9).
- 711 Earth Resources Observation and Science (EROS) Center. 2022. *Landsat Collection 2 Level-3 Dynamic  
Surface Water Extent Science Product*.
- 714 European Space Agency (ESA). 2017. “The Climate Change Initiative Land Cover (CCI-LC) Dataset .”  
Retrieved August 14, 2015 (<http://maps.elie.ucl.ac.be/CCI/viewer/download.php>).
- Fountain, Andrew G., and Wendell V. Tangborn. 1985. “The Effect of Glaciers on Streamflow  
Variations.” *Water Resources Research* 21(4). doi: 10.1029/WR021i004p00579.
- 717 Garreaud, René D., Camila Alvarez-Garreton, Jonathan Barichivich, Juan Pablo Boisier, Duncan  
Christie, Mauricio Galleguillos, Carlos LeQuesne, James McPhee, and Mauricio Zambrano-





- 720 Bigiarini. 2017. "The 2010-2015 Megadrought in Central Chile: Impacts on Regional Hydroclimate and Vegetation." *Hydrology and Earth System Sciences* 21(12). doi: 10.5194/hess-21-6307-2017.
- 723 Gelman, Andrew, and Jennifer Hill. 2007. "Data Analysis Using Regression and Multilevel/Hierarchical Models." *Cambridge University Press* 30(April).
- 726 Guardiola-Claramonte, M., Peter A. Troch, David D. Breshears, Travis E. Huxman, Matthew B. Switanek, Matej Durcik, and Neil S. Cobb. 2011. "Decreased Streamflow in Semi-Arid Basins Following Drought-Induced Tree Die-off: A Counter-Intuitive and Indirect Climate Impact on Hydrology." *Journal of Hydrology* 406(3–4). doi: 10.1016/j.jhydrol.2011.06.017.
- 729 Gudmundsson, Lukas, Hong Xuan Do, Michael Leonard, and Seth Westra. 2018. "The Global Streamflow Indices and Metadata Archive (GSIM)-Part 2: Quality Control, Time-Series Indices and Homogeneity Assessment." *Earth System Science Data* 10(2). doi: 10.5194/essd-10-787-2018.
- 732 Van Huijgevoort, M. H. J., P. Hazenberg, H. A. J. Van Lanen, and R. Uijlenhoet. 2012. "A Generic Method for Hydrological Drought Identification across Different Climate Regions." *Hydrology and Earth System Sciences* 16(8):2437–51. doi: 10.5194/hess-16-2437-2012.
- 735 Klockow, Paul A., Jason G. Vogel, Christopher B. Edgar, and Georgianne W. Moore. 2018. "Lagged Mortality among Tree Species Four Years after an Exceptional Drought in East Texas." *Ecosphere* 9(10). doi: 10.1002/ecs2.2455.
- 738 Lamontagne-Hallé, Pierrick, Jeffrey M. McKenzie, Barret L. Kurylyk, and Samuel C. Zipper. 2018. "Changing Groundwater Discharge Dynamics in Permafrost Regions." *Environmental Research Letters* 13(8). doi: 10.1088/1748-9326/aad404.
- 741 Levy, M. C., A. V. Lopes, A. Cohn, L. G. Larsen, and S. E. Thompson. 2018. "Land Use Change Increases Streamflow Across the Arc of Deforestation in Brazil." *Geophysical Research Letters* 45(8). doi: 10.1002/2017GL076526.
- 744 Liu, Qiang, Liqiao Liang, Tao Sun, Xuan Wang, Chunhui Li, and Sirui Yan. 2023. "Assessment of the Shift in the Precipitation–Streamflow Relationship Influenced by Multiyear Drought, Yellow River Basin, China." *Science of the Total Environment* 903. doi: 10.1016/j.scitotenv.2023.166203.
- 747 Liu, Qiang, Yuting Yang, Liqiao Liang, Denghua Yan, Xuan Wang, Chunhui Li, and Tao Sun. 2022. "Shift in Precipitation-Streamflow Relationship Induced by Multi-Year Drought across Global Catchments." *Science of the Total Environment* 857. doi: 10.1016/j.scitotenv.2022.159560.
- 750 Liu, Xuqing, Feng Gao, Yandong Wu, and Zhiguo Zhao. 2018. "Detecting Outliers and Influential Points: An Indirect Classical Mahalanobis Distance-Based Method." *Journal of Statistical Computation and Simulation* 88(11). doi: 10.1080/00949655.2018.1448981.
- 753 Liu, Yanghe, Pan Liu, Lu Zhang, Xiaojing Zhang, Yunfan Zhang, and Lei Cheng. 2021. "Detecting and Attributing Drought-Induced Changes in Catchment Hydrological Behaviours in a Southeastern Australia Catchment Using a Data Assimilation Method." *Hydrological Processes* 35(7). doi: 10.1002/hyp.14289.
- 756 Van Loon, A. F., and G. Laaha. 2015. "Hydrological Drought Severity Explained by Climate and Catchment Characteristics." *Journal of Hydrology* 526. doi: 10.1016/j.jhydrol.2014.10.059.



- 759 Van Loon, Anne F. 2015. "Hydrological Drought Explained." *WIREs Water* 2(4). doi:  
10.1002/wat2.1085.
- 762 Lutz, A. F., W. W. Immerzeel, A. B. Shrestha, and M. F. P. Bierkens. 2014. "Consistent Increase in High  
Asia's Runoff Due to Increasing Glacier Melt and Precipitation." *Nature Climate Change* 4(7). doi:  
10.1038/nclimate2237.
- 765 Martens, Brecht, Diego G. Miralles, Hans Lievens, Robin Van Der Schalie, Richard A. M. De Jeu, Diego  
Fernández-Prieto, Hylke E. Beck, Wouter A. Dorigo, and Niko E. C. Verhoest. 2017. "GLEAM v3:  
Satellite-Based Land Evaporation and Root-Zone Soil Moisture." *Geoscientific Model  
Development* 10(5). doi: 10.5194/gmd-10-1903-2017.
- 768 Massari, Christian, Francesco Avanzi, Giulia Bruno, Simone Gabellani, Daniele Penna, and Stefania  
Camici. 2022. "Evaporation Enhancement Drives the European Water-Budget Deficit during  
Multi-Year Droughts." *Hydrology and Earth System Sciences* 26(6). doi: 10.5194/hess-26-1527-  
771 2022.
- 774 Matanó, Alessia, Wouter R. Berghuijs, Maurizio Mazzoleni, Marleen C. de Ruyter, Philip J. Ward, and  
Anne F. Van Loon. 2024. "Compound and Consecutive Drought-Flood Events at a Global Scale."  
*Environmental Research Letters* 19(6). doi: 10.1088/1748-9326/ad4b46.
- 777 Maurer, Tessa, Francesco Avanzi, Steven D. Glaser, and Roger C. Bales. 2022. "Drivers of Drought-  
Induced Shifts in the Water Balance through a Budyko Approach." *Hydrology and Earth System  
Sciences* 26(3):589–607. doi: 10.5194/hess-26-589-2022.
- Moody, Carlisle E. 2017. "Fixed-Effects Panel Data Models: To Cluster or Not to Cluster." *SSRN  
Electronic Journal*. doi: 10.2139/ssrn.2840273.
- 780 NOAA. 2022. "Star - Global Vegetation Health Products [Dataset]." Retrieved August 12, 2022  
([https://www.star.nesdis.noaa.gov/smcd/emb/vci/VH/vh\\_ftp.php](https://www.star.nesdis.noaa.gov/smcd/emb/vci/VH/vh_ftp.php)).
- 783 Pan, Zhengke, Pan Liu, Chong Yu Xu, Lei Cheng, Jing Tian, Shujie Cheng, and Kang Xie. 2020. "The  
Influence of a Prolonged Meteorological Drought on Catchment Water Storage Capacity: A  
Hydrological-Model Perspective." *Hydrology and Earth System Sciences* 24(9). doi:  
10.5194/hess-24-4369-2020.
- 786 Paparoditis, Efstathios, and Dimitris N. Politis. 2018. "The Asymptotic Size and Power of the  
Augmented Dickey–Fuller Test for a Unit Root." *Econometric Reviews* 37(9). doi:  
10.1080/00927872.2016.1178887.
- 789 Parry, Simon, Christel Prudhomme, Robert L. Wilby, and Paul J. Wood. 2016. "Drought Termination:  
Concept and Characterisation." *Progress in Physical Geography* 40(6). doi:  
10.1177/0309133316652801.
- 792 Peterson, Tim J., M. Saft, M. C. Peel, and A. John. 2021. "Watersheds May Not Recover from Drought."  
*Science* 372(6543). doi: 10.1126/science.abd5085.
- 795 Rodrigues, Regina R., and Michael J. McPhaden. 2014. "Why Did the 2011–2012 La Niña Cause a  
Severe Drought in the Brazilian Northeast?" *Geophysical Research Letters* 41(3). doi:  
10.1002/2013GL058703.
- 798 Rubel, Franz, and Markus Kottek. 2010. "Observed and Projected Climate Shifts 1901–2100 Depicted  
by World Maps of the Köppen–Geiger Climate Classification." *Meteorologische Zeitschrift* 19(2).  
doi: 10.1127/0941-2948/2010/0430.



- 801 Saft, Margarita, Murray C. Peel, Andrew W. Western, Jean Michel Perraud, and Lu Zhang. 2016. "Bias in Streamflow Projections Due to Climate-Induced Shifts in Catchment Response." *Geophysical Research Letters* 43(4). doi: 10.1002/2015GL067326.
- 804 Saft, Margarita, Murray C. Peel, Andrew W. Western, and Lu Zhang. 2016. "Predicting Shifts in Rainfall-Runoff Partitioning during Multiyear Drought: Roles of Dry Period and Catchment Characteristics." *Water Resources Research* 52(12). doi: 10.1002/2016WR019525.
- 807 Saft, Margarita, Andrew W. Western, Lu Zhang, Murray C. Peel, and Nick J. Potter. 2015. "The Influence of Multiyear Drought on the Annual Rainfall-Runoff Relationship: An Australian Perspective." *Water Resources Research* 51(4). doi: 10.1002/2014WR015348.
- 810 Sakia, R. M. 1992. "The Box-Cox Transformation Technique: A Review." *The Statistician* 41(2). doi: 10.2307/2348250.
- 813 Santos, Léonard, Guillaume Thirel, and Charles Perrin. 2018. "Technical Note: Pitfalls in Using Log-Transformed Flows within the KGE Criterion." *Hydrology and Earth System Sciences* 22(8). doi: 10.5194/hess-22-4583-2018.
- 816 Schaner, Neil, Nathalie Voisin, Bart Nijssen, and Dennis P. Lettenmaier. 2012. "The Contribution of Glacier Melt to Streamflow." *Environmental Research Letters* 7(3). doi: 10.1088/1748-9326/7/3/034029.
- 819 van Tiel, Marit, Caroline Aubry-Wake, Lauren Somers, Christoff Andermann, Francesco Avanzi, Michel Baraer, Gabriele Chiogna, Clémence Daigre, Soumik Das, Fabian Drenkhan, Daniel Farinotti, Catriona L. Fyffe, Inge de Graaf, Sarah Hanus, Walter Immerzeel, Franziska Koch, Jeffrey M. McKenzie, Tom Müller, Andrea L. Popp, Zarina Saidaliyeva, Bettina Schaefli, Oliver S. Schilling, Kapiolani Teagai, James M. Thornton, and Vadim Yapiyev. 2024. "Cryosphere–Groundwater Connectivity Is a Missing Link in the Mountain Water Cycle." *Nature Water* 2(7):624–37. doi: 10.1038/s44221-024-00277-8.
- 822
- 825 Urgeghe, Anna M., David D. Breshears, Scott N. Martens, and Peter C. Beeson. 2010. "Redistribution of Runoff among Vegetation Patch Types: On Ecohydrological Optimality of Herbaceous Capture of Run-On." *Rangeland Ecology and Management* 63(5). doi: 10.2111/REM-D-09-00185.1.
- 828 Wagenmakers, Eric Jan, and Simon Farrell. 2004. "AIC Model Selection Using Akaike Weights." *Psychonomic Bulletin and Review* 11(1).
- 831 Wasko, Conrad, Rory Nathan, and Murray C. Peel. 2020. "Trends in Global Flood and Streamflow Timing Based on Local Water Year." *Water Resources Research* 56(8). doi: 10.1029/2020WR027233.
- 834 Wu, Jiefeng, Xiaohong Chen, Xing Yuan, Huaxia Yao, Yunxia Zhao, and Amir AghaKouchak. 2021. "The Interactions between Hydrological Drought Evolution and Precipitation-Streamflow Relationship." *Journal of Hydrology* 597. doi: 10.1016/j.jhydrol.2021.126210.
- 837 Zhang, Xia, Mingxing Li, Zhuguo Ma, Qing Yang, Meixia Lv, and Robin Clark. 2019. "Assessment of an Evapotranspiration Deficit Drought Index in Relation to Impacts on Ecosystems." *Advances in Atmospheric Sciences* 36(11). doi: 10.1007/s00376-019-9061-6.